0026-895X/92/061069-08$03.00/0

MOLECULAR PHARMACOLOGY, 42:1069-1076

Binding Kinetics of γ-Aminobutyric Acid$_A$ Receptor Noncompetitive Antagonists: Trioxabicyclooctane, Dithiane, and Cyclodiene Insecticide-Induced Slow Transition to Blocked Chloride Channel Conformation

JON E. HAWKINSON[1] and JOHN E. CASIDA

Pesticide Chemistry and Toxicology Laboratory, Department of Entomological Sciences, University of California, Berkeley, California 94720

Received July 31, 1992; Accepted September 29, 1992

SUMMARY

Binding kinetics and affinities are determined for 25 antagonists interacting with the noncompetitive blocker site of the γ-aminobutyric acid$_A$ receptor complex present in bovine brain membranes. Four radiolabeled noncompetitive antagonists are 4-*tert*-butylbicyclophosphoro[^{35}S]thionate ([^{35}S]TBPS), 4-*tert*-butylbicycloortho[3′,4′-$^3H_2$]benzoate, 4′-cyano-4-*sec*-[3,4-$^3H_2$]butylbicycloorthobenzoate, and the new 4′-ethynyl-4-*n*-[2,3-$^3H_2$]propylbicycloorthobenzoate. The other 21 antagonists are unlabeled inhibitors of three chemical classes (other trioxabicyclooctane, dithiane, and cyclodiene insecticides). The radioligands bind to a single noninteracting site in the membranes, based on linear Scatchard plots and monophasic association and dissociation kinetics. The kinetics of unlabeled ligands are estimated by their effect on the [^{35}S]TBPS association curve, using the theoretical model of Motulsky and Mahan [*Mol. Pharmacol.* **25**:1-9 (1984)]. The receptor affinities of trioxabicyclooctanes and dithianes correlate with their association rates, whereas those of cyclodienes correlate with their dissociation rates. The low association rate constants for all ligands ($\leq 3 \times 10^7$ M^{-1} min^{-1} at 25°) are consistent with a slow transition to a blocked receptor conformation upon binding of these channel blockers. The association rate-controlled affinity for the trioxabicyclooctanes and dithianes is suggestive of an induced-fit model in which binding of the ligand initiates a conformational change in the receptor complex to the blocked state.

The GABA$_A$ receptor is a major target for convulsants and insecticides that noncompetitively antagonize the action of GABA, the main inhibitory neurotransmitter in mammalian brain (1, 2). The three most potent classes of compounds acting as NCBs of the GABA-gated chloride channel are TBOs including both bicyclophosphorus esters and bicycloorthobenzoates, dithianes and their *S*-oxidation products, and selected cyclodiene insecticides (3) (Fig. 1). These convulsants bind the mammalian brain GABA$_A$ receptor at a site distinct from that for GABA, termed the NCB site. Occupancy of the NCB site inhibits GABA-stimulated $^{36}Cl^-$ flux, consistent with blockade of the integral chloride channel (4).

The pharmacological profile and the toxicological relevance of the NCB site are defined primarily by studies using four TBO radioligands, i.e., [^{35}S]TBPS (5), [^{3}H]TBOB (6), [^{3}H]CNsBOB (7), and [^{3}H]EBOB (8) (Fig. 1). Knowledge of the binding kinetics is restricted to these TBO radioligands. The binding kinetics of unlabeled ligands are generally unknown. Thus, no kinetic information exists for unlabeled TBO, dithiane, or cyclodiene ligands.

The present study examines the kinetics of unlabeled ligands by their effect on the [^{35}S]TBPS association curve. This procedure is based on the theoretical model of Motulsky and Mahan (9) developed for β-adrenergic ligands by Contreras *et al.* (10). It is validated for the GABA$_A$ receptor NCB site by comparison of results for the three bicycloorthobenzoate radioligands with those for the same compounds in unlabeled form. This [^{35}S]TBPS coincubation method with bovine brain GABA$_A$ receptor allows for the first time the definition of the kinetics of unlabeled TBO, dithiane, and cyclodiene binding to the NCB site.

Materials and Methods

Chemicals. Structures and designations of the radioligands and inhibitors are shown in Fig. 1. [^{35}S]TBPS (61-134 Ci/mmol) was

This work was supported in part by National Institutes of Health Grant 5 PO1 ES00049 and was presented at the 31st Annual Meeting of the Society of Toxicology, Seattle, WA, 1992 (42).

[1] Present address: CoCensys, 213 Technology Drive, Irvine, CA 92718.

ABBREVIATIONS: GABA, γ-aminobutyric acid; [^{35}S]TBPS, 4-*tert*-butylbicyclophosphoro[^{35}S]thionate; [^{3}H]TBOB, 4-*tert*-butylbicycloortho[3′,4′-$^3H_2$]benzoate; [^{3}H]CNsBOB, 4′-cyano-4-*sec*-[3,4-$^3H_2$]butylbicycloorthobenzoate; [^{3}H]EBOB, 4′-ethynyl-4-*n*-[2,3-$^3H_2$]propylbicycloorthobenzoate; TBO, trioxabicyclooctane; NCB, noncompetitive blocker.

obtained from DuPont/New England Nuclear and [^{3}H]TBOB (30 Ci/mmol) from Amersham Corp. [^{3}H]CNsBOB (theoretical specific activity, 60 Ci/mmol) (7) and [^{3}H]EBOB (60 Ci/mmol) (11) were synthesized by reduction of the olefinic precursors with tritium gas.

Synthesis and properties of the TBOs examined (Fig. 1) were described previously, as follows: TBPS and TBPO (12); TBPSe (by a method similar to that for TBPS) (12); TBOB, 4′-Br-TBOB, and 4′-CN-TBOB (13); 4′-Br-3′,5′-Cl_2-TBOB (14); 3-CN-4′-ethynyl-TBOB (15); F-phenyl-EBOB (16); CNsBOB (7); and EBOB (17). The dithianes and their *S*-oxidation products were prepared in this laboratory (18). The cyclodienes studied were as reported previously (19).

Because the TBOs are hydrolytically unstable (20), their purity was verified by NMR before use. The hydrolysis rates of unlabeled EBOB and CNsBOB (10–20 μM) were determined in the binding buffer (described below) at 25°. This involved monitoring the time-dependent increase in absorbance of their benzoate ester hydrolysis products at 260 and 242 nm, respectively.

Membrane preparation. EDTA-dialyzed bovine brain membranes were prepared as previously described (14), with modifications. Portions of cerebral cortex (stored at −70°) were thawed and homogenized with a Teflon/glass homogenizer in 10 volumes of ice-cold 0.32 M sucrose. The homogenate was centrifuged at 1000 × *g* for 10 min at 4° and the supernatant was then centrifuged at 17,000 × *g* for 20 min. The resultant pellet was resuspended in 1 mM EDTA/50 mM Tris·HCl (pH 7.5), dialyzed against 3 volumes of deionized water for 5 hr, and then centrifuged at 33,000 × *g* for 30 min. The final pellet was resuspended in 50 mM Tris·HCl (pH 7.5) at 8 mg of protein/ml and was stored at −70°. Before use, the membranes were thawed, homogenized, and diluted in 50 mM Tris·HCl (pH 7.5).

Binding assays. Each radioligand was independently incubated with brain membranes [0.2–0.4 mg of protein, measured by a modified Lowry procedure (21), with bovine serum albumin as the standard] in 1 ml of 500 mM KBr/50 mM Tris·HCl (pH 7.5) at 25°. In optimization by others, the highest levels of [^{35}S]TBPS binding were observed at ~500 mM KBr (22) and subphysiological temperature (5), and high salt concentrations are also required for optimal [^{3}H]TBOB binding (6). Binding was terminated by filtration through GF/C filters using a 24-place cell harvester (Brandel), followed by rinsing with ice-cold buffer (3 × 4 ml) and liquid scintillation counting. Specific binding was determined using 4 μM unlabeled TBOB for [^{35}S]TBPS and 4 μM unlabeled TBPS for [^{3}H]TBOB, [^{3}H]EBOB, and [^{3}H]CNsBOB and was 93, 72, 91, and 77% at 1 nM concentrations, respectively. All assays were run in duplicate.

Saturation, competition, and kinetic experiments. In saturation assays, each radioligand was incubated with membranes for 3 hr. The specific activity of [^{35}S]TBPS was diluted with unlabeled TBPS, followed by incubation with 10 levels of the "hot/cold" mixture. Ten concentrations of the ^{3}H-radioligands were also used with only labeled compound.

In competition assays, inhibitors at five concentrations resulting in 10–90% inhibition were added in 5 μl of dimethylsulfoxide and incubated with 2 nM [^{35}S]TBPS and membranes for 3 hr.

For direct determination of association rate constants, radioligands were incubated for increasing times up to 60 min (120 min for [^{35}S]TBPS) at 2–4 nM. For association assays with unlabeled ligands, [^{35}S]TBPS was coincubated with an inhibitor added in dimethylsulfoxide (final concentration, 0.02%) at approximately an IC_{50} level, the concentration of ligand giving 50% inhibition of specific binding.

For dissociation assays, after incubation with the radioligand at 1–4 nM to approximate equilibrium (90 min for [^{35}S]TBPS; 30–60 min for [^{3}H]TBOB, [^{3}H]CNsBOB, and [^{3}H]EBOB) excess identical ligand in unlabeled form (4 μM) was added to block reassociation of the radioligand, and suspensions were filtered at various times (0–92 min, depending on the radioligand).

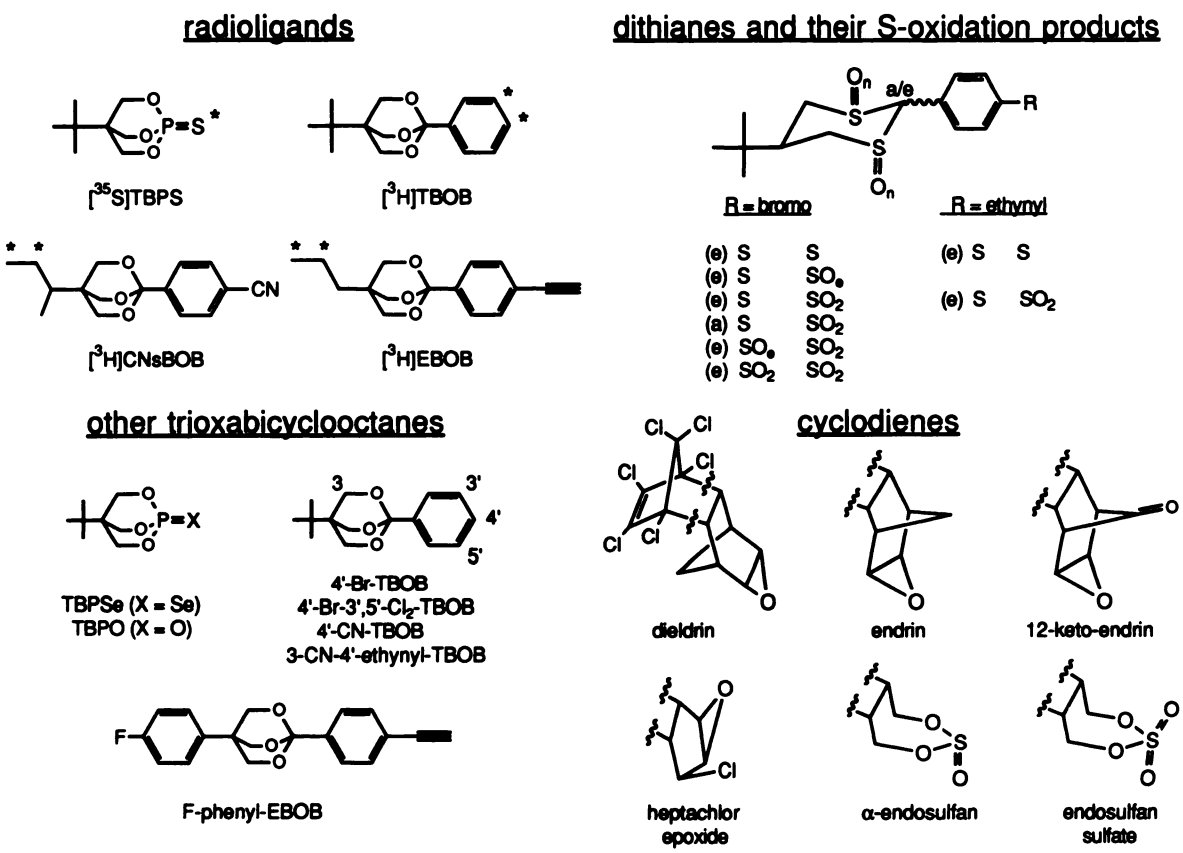

Fig. 1. Structures and designations of radioligands and inhibitors. Complete structure is shown for dieldrin and partial structures are shown for the other cyclodienes.

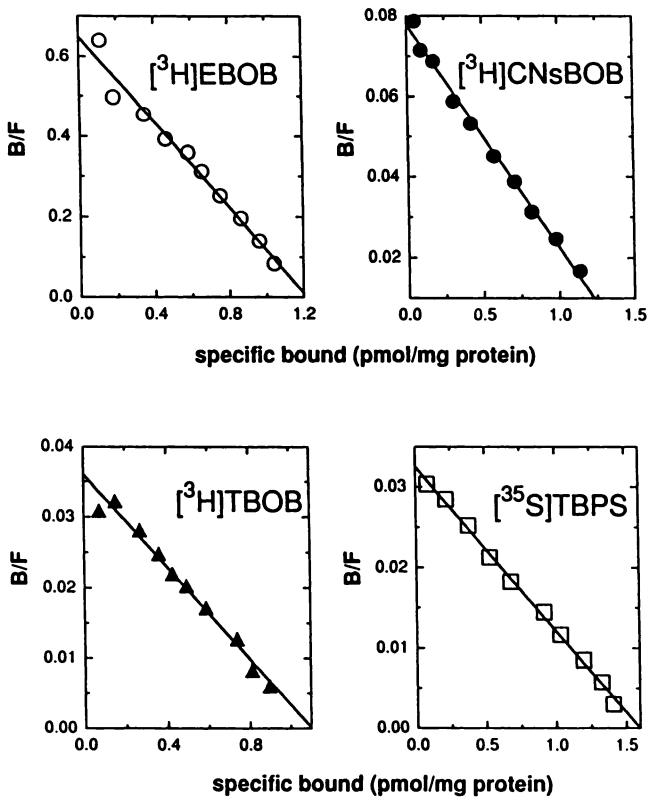

Fig. 2. Scatchard plots of saturation analyses of four radioligands binding to bovine brain membranes. Bovine brain membranes (250 μg) were incubated with 10 concentrations of the radioligand indicated for 3 hr at 25°. Each plot represents one of two independent experiments used to calculate the K_d and B_{max} values (Table 1) with the EBDA computer program.

Data analysis. According to the law of mass action, the binding of the radioligand (L) to the receptor (R) is given by eq. 1, where k_1 and k_2 are the rate constants of association and dissociation, respectively, and K_d is the dissociation constant for the radioligand.

$$L + R \underset{k_2}{\overset{k_1}{\rightleftharpoons}} LR$$

$$K_d = \frac{[LR]}{[L]\,[R]} = \frac{k_2}{k_1} \quad (1)$$

For equilibrium measurements, the K_d values and maximal binding capacities (B_{max} values) for the radioligands were determined by Scatchard transformations of equilibrium binding data using the EBDA computer program (Biosoft). Inhibition constants (K_i values) for unlabeled inhibitors were calculated from IC_{50} values using the EBDA program and the equation of Cheng and Prusoff (23) (eq. 2).

$$K_i = \frac{IC_{50}}{1 + \frac{[L]}{K_d}} \quad (2)$$

Kinetic constants for radioligands were calculated by three methods. In method A, the standard approach, the off-rate k_2 was determined from the slope of first-order radioligand dissociation after addition of excess unlabeled ligand, using the KINETIC computer program (Biosoft) and eq. 3, where B is the amount bound at any time t and B_0 is the amount bound at $t = 0$.

$$\frac{B}{B_0} = e^{-k_2 t} \quad (3)$$

The observed on-rate (k_{obs}) was determined from the pseudo-first-order function (eq. 4) using EBDA, where B_e is the amount bound at equilibrium.

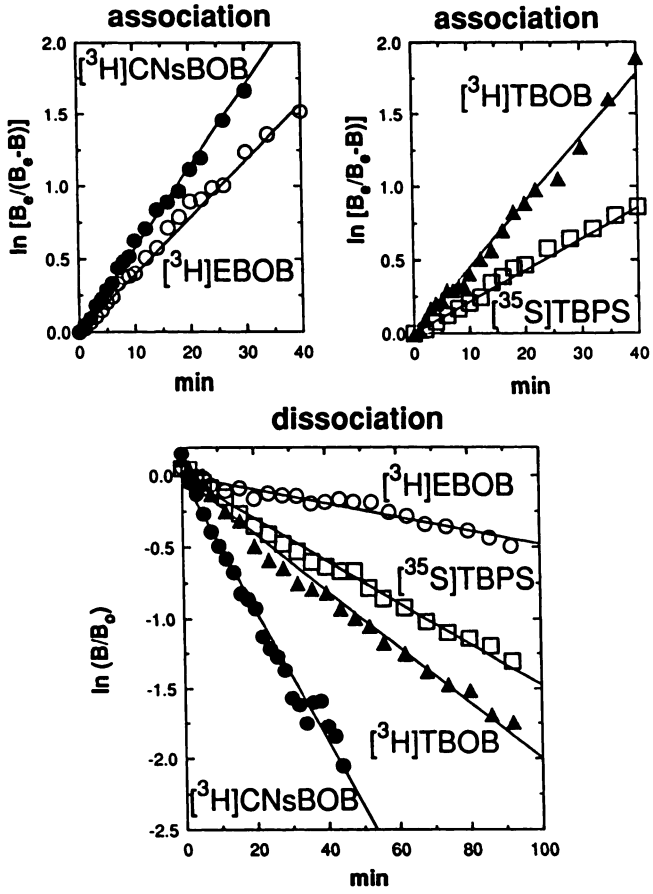

Fig. 3. Kinetic analyses of four radioligands binding to bovine brain membranes. For association experiments, radioligands (2–4 nM) were incubated with bovine brain membranes (250 μg) at 25° for the time indicated. See Fig. 4 for [^{35}S]TBPS association curve (control). For dissociation experiments, radioligands (1–4 nM) were incubated with bovine brain membranes (250 μg) at 25° for 30–90 min, followed by addition of excess unlabeled ligand (4 μM) to initiate dissociation. Each *line* is a pseudo-first-order (association) or first-order (dissociation) plot (method A) from one of two or three independent experiments used to calculate the K_1 and k_2 values (Table 1) with the KINETIC computer program.

$$\frac{B_e}{B_e - B} = e^{(k_{obs} \cdot t)} \quad (4)$$

The on-rate k_1 was estimated according to eq. 5, where L_T is the total radioligand concentration, and the kinetic dissociation constant (k_2/k_1) was then calculated using eq. 1.

$$k_1 = \frac{k_{obs} - k_2}{L_T} \quad (5)$$

In method B, the on-rate was calculated using a second-order function (eq. 6) according to the method of Contreras *et al.* (10), using the ENZFITTER computer program (Elsevier-Biosoft), where R_T is the total concentration of receptor determined by Scatchard analysis.

$$\ln \frac{B_e\left[L_T - \frac{(B \cdot B_e)}{R_T}\right]}{L_T(B_e - B)} = (k_1)\,(t)\left[\frac{(L_T \cdot R_T)}{B_e} - B_e\right] \quad (6)$$

The kinetic K_d (k_2/k_1) was then determined using the k_2 from dissociation experiments and eq. 1, as in method A. In method C, both rate constants were calculated simultaneously by fitting the association

TABLE 1

Saturation and kinetic parameters for the binding of TBO radioligands to bovine brain membranes

Experimental details are given in Figs. 2 and 3 and Materials and Methods.

Radioligand	Saturation parameters[a]			Kinetic parameters		
	K_d	B_{max}	Method[b]	k_1	k_2	k_2/k_1
	nM	pmol/mg of protein		10^6 M^{-1} min^{-1}	min^{-1}	nM
[^{3}H]EBOB	0.43 ± 0.05	1.27 ± 0.05	A	15 ± 4	0.0044 ± 0.0007	0.32 ± 0.06
			B	18 ± 3		0.25 ± 0.04
			C	18 ± 3	0.010 ± 0.002	0.6 ± 0.2
[^{3}H]CNsBOB	3.9 ± 0.3	1.46 ± 0.05	A	2.4[c]	0.052 ± 0.006	22
			B	7.48 ± 0.02		6.98 ± 0.02
			C	7.49 ± 0.02	0.0440 ± 0.001	5.86 ± 0.03
[^{3}H]TBOB	6.0 ± 0.1	1.12 ± 0.02	A	5.6 ± 0.5	0.022 ± 0.002	3.9 ± 0.4
			B	3.9 ± 0.2		5.5 ± 0.3
			C	3.9 ± 0.2	0.0265 ± 0.0001	6.8 ± 0.3
[^{35}S]TBPS	19.8 ± 0.03	1.601 ± 0.001	A	1.8 ± 0.6	0.0153 ± 0.0004	11 ± 4
			B	0.99 ± 0.01		15.6 ± 0.2
			C	0.99 ± 0.01	0.021 ± 0.001	21.4 ± 0.7

[a] K_d and B_{max} values (means ± standard errors) were calculated from Scatchard plots of saturation data from two independent experiments.

[b] Method A is the standard calculation of kinetic data from separate association and dissociation experiments (two or three independent experiments each) (means ± standard errors). Method B is a second-order treatment of the association data to estimate k_1 (means ± standard errors). Method C is a pseudo-first-order treatment of the association data to estimate k_1 and k_2 simultaneously (means ± standard errors).

[c] A single value is reported because for the replicate experiment k_2 was greater than k_{obs}, making k_1 negative according to eq. 5.

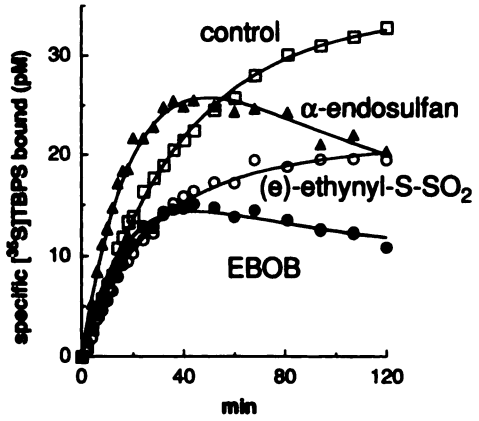

Fig. 4. Determination of kinetic constants for unlabeled ligands from [^{35}S] TBPS association curves. Unlabeled ligands were coincubated with [^{35}S] TBPS and bovine brain membranes for increasing times up to 120 min. All data are from single experiments. The control curve was fitted using method C (eq. 7) and the curves in the presence of unlabeled inhibitors were fitted using the Motulsky and Mahan (9) equation (eq. 9), in each case with the ENZFITTER computer program. [^{35}S]TBPS k_1 and k_2 values used to calculate kinetic constants of unlabeled inhibitors are 0.99×10^6 M^{-1} and 0.021 min^{-1}, respectively, and R_T for all experiments is 400 pM. Conditions for individual experiments were: control, L_T = 2.1 nM; EBOB, L_T = 2.8 nM, I_T = 2 nM; (e)-ethynyl-S-SO$_2$, L_T = 2.1 nM, I_T = 1 nM; α-endosulfan, L_T = 4.1 nM, I_T = 15 nM.

data to a pseudo-first-order function (eq. 7) using ENZFITTER, where the pseudo-first-order rate constant $K_A = k_1(L_T) + k_2$ (10).

$$B = \frac{k_1 \cdot R_T \cdot L_T}{K_A}[1 - e^{-(K_A \cdot t)}] \quad (7)$$

Kinetic constants for unlabeled ligands were determined in coincubation experiments in which the association curve for [^{35}S]TBPS was determined in the presence of the competitive inhibitor (I). In this case, the radioligand binds the receptor according to eq. 1 simultaneously with binding of I, given by eq. 8.

$$I + R \underset{k_4}{\overset{k_3}{\rightleftharpoons}} IR \quad (8)$$

Using eqs. 1 and 8 and $R_T = R_F + [LR] + [IR]$, where R_F, $[LR]$, and $[IR]$ are the concentrations of free receptor, radioligand receptor complex, and inhibitor receptor complex, respectively, Motulsky and Mahan (9) derived a pseudo-first-order function (eq. 9) that is valid if <10% of the inhibitor and radioligand are bound, where K_A, K_B, K_F, and K_S are as in eq. 10 and I_T is the total inhibitor concentration.

$$B = \frac{R_T \cdot k_1 \cdot L_T}{K_F - K_S}\left[\frac{k_4(K_F - K_S)}{K_F \cdot K_S} + \frac{(k_4 - K_F)}{K_F}e^{-(K_F \cdot t)} - \frac{(k_4 - K_S)}{K_S}e^{-(K_S \cdot t)}\right] \quad (9)$$

$$K_A = k_1 L_T + k_2$$

$$K_B = k_3 I_T + k_4$$

$$K_F = 0.5[K_A + K_B + \sqrt{(K_A - K_B)^2 + 4\,k_1 k_3 L_T I_T}] \quad (10)$$

$$K_S = 0.5[K_A + K_B - \sqrt{(K_A - K_B)^2 + 4k_1 k_3 L_T I_T}]$$

After determination of R_T from Scatchard analysis and k_1 and k_2 using method C, the rate constants for unlabeled inhibitors were calculated from eq. 9 using ENZFITTER. The kinetic dissociation constant for the inhibitors was calculated as k_4/k_3.

Results

Saturation parameters for four TBO radioligands. Scatchard plots reveal a single class of noninteracting binding sites and similar binding capacities for each radioligand (Fig. 2). The order of affinity is [^{3}H]EBOB ≫ [^{3}H]CNsBOB > [^{3}H]TBOB > [^{35}S]TBPS (Table 1).

Association rates for four TBO radioligands. The association of all four radioligands is linear on pseudo-first-order plots (Fig. 3) and ranges from 1 to 18 × 10^6 M^{-1} min^{-1} for [^{35}S]TBPS and [^{3}H]EBOB, respectively (Table 1). Analysis of the association data using methods B and C gives almost identical estimations of the on-rates for all four radioligands, but use of the standard approach (method A) results in discrepancies from the other methods of 1.2-, 1.4-, 1.8-, and 3.1-fold for [^{3}H]EBOB, [^{3}H]TBOB, [^{35}S]TBPS, and [^{3}H]CNsBOB, respectively. Thus, up to 3-fold differences in on-rate estimates are obtained using different models applied to identical data sets. This is largely due to the situation when the absolute values of the experimentally derived k_2 and k_{obs} terms used in eq. 5 are close, leading to large errors in the calculated k_1. This weakness in the

TABLE 2

Kinetic and inhibition constants for the binding of unlabeled inhibitors to bovine brain membranes using [^{35}S]TBPS as radioligand

Experimental details are given in Fig. 4 and Materials and Methods

No.	Unlabeled ligand	K_i[a]	Kinetic parameters[b]		
			k_3	k_4	k_4/k_3
		nM	10^6 M^{-1} min^{-1}	min^{-1}	nM
	TBOs for which radiolabeled form is available				
1	EBOB	1.1 ± 0.1	17 ± 4	0.012 ± 0.001	0.76 ± 0.23
2	CNsBOB	4.4 ± 0.3	12 ± 1	0.040 ± 0.002	3.4 ± 0.2
3	TBOB	11.1 ± 0.1	4.0 ± 0.5	0.040 ± 0.003	10.2 ± 0.5
4	TBPS	24 ± 3			
	Other TBOs				
5	3-CN-4′-ethynyl-TBOB	0.67 ± 0.09	20 ± 1	0.014 ± 0.008	0.67 ± 0.35
6	F-phenyl-EBOB	1.3 ± 0.1	24 ± 8	0.027 ± 0.005	1.2 ± 0.2
7	4′-Br-3′,5′-Cl$_2$-TBOB	1.5 ± 0.1	6 ± 3	0.016 ± 0.004	3.2 ± 1.1
8	4′-CN-TBOB	1.6 ± 0.3	13 ± 5	0.022 ± 0.003	1.9 ± 0.5
9	4′-Br-TBOB	1.8 ± 0.2	10 ± 1	0.017 ± 0.004	1.8 ± 0.5
10	TBPSe	32 ± 3	2.8 ± 0.6	0.087 ± 0.010	31 ± 3
11	TBPO	117 ± 2	0.18 ± 0.01	0.026 ± 0.004	145 ± 25
	Dithianes and their *S*-oxidation products				
12	(*e*)-Ethynyl-S-SO$_2$	1.53 ± 0.02	26 ± 2	0.038 ± 0.001	1.4 ± 0.1
13	(*e*)-Ethynyl-S-S	3.5 ± 0.2	6 ± 1	0.03 ± 0.01	5 ± 1
14	(*a*)-Br-S-SO$_2$	6.7 ± 0.7	17.5 ± 0.1	0.106 ± 0.002	6.1 ± 0.1
15	(*e*)-Br-SO$_2$-SO$_2$	8.2 ± 0.4	2.6 ± 0.3	0.020 ± 0.004	7.6 ± 0.7
16	(*e*)-Br-S-SO$_2$	9.7 ± 0.5	14 ± 6	0.11 ± 0.04	8.0 ± 0.2
17	(*e*)-Br-S-SO$_e$	16.1 ± 0.1	9.9 ± 0.8	0.17 ± 0.03	17 ± 2
18	(*e*)-Br-SO$_e$-SO$_2$	30 ± 2	1.42 ± 0.02	0.043 ± 0.002	30 ± 1
19	(*e*)-Br-S-S	66 ± 3	2.2 ± 0.5	0.17 ± 0.10	71 ± 29
	Cyclodienes				
20	12-Ketoendrin	5 ± 2	7.5 ± 0.2	0.017 ± 0.001	2.2 ± 0.2
21	α-Endosulfan	6.3 ± 0.1	1.64 ± 0.04	0.012 ± 0.006	7 ± 4
22	Endrin	7.46 ± 0.004	1.4 ± 0.4	0.0113 ± 0.0001	9 ± 2
23	Endosulfan sulfate	7.7 ± 0.3	4.2 ± 1.8	0.023 ± 0.005	6 ± 1
24	Heptachlor epoxide	51 ± 5	2.4 ± 1.0	0.13 ± 0.04	56 ± 7
25	Dieldrin	73 ± 11	1.06 ± 0.03	0.088 ± 0.018	84 ± 19

[a] Inhibition constant K_i (mean ± standard error) of two independent experiments was calculated from competition data (five inhibitor concentrations incubated to equilibrium).

[b] Kinetic constants k_3 and k_4 (mean ± standard error of two independent experiments) were determined by analysis of [^{35}S]TBPS association time course data in the presence of a single concentration of inhibitor, using the equation of Motulsky and Mahan (9).

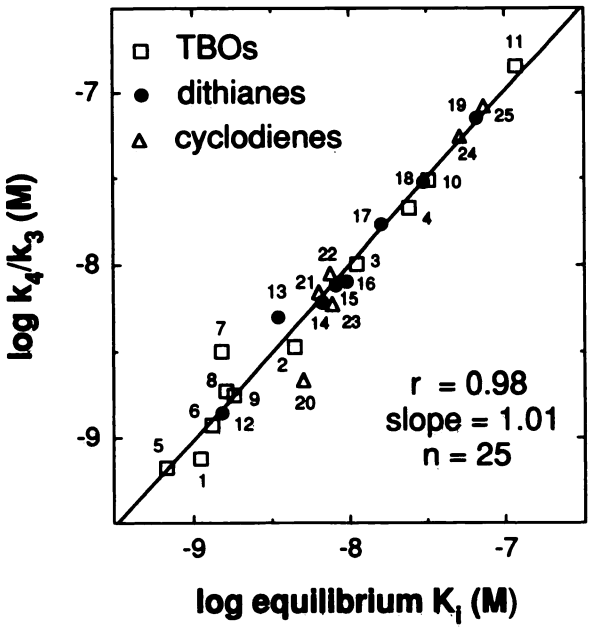

Fig. 5. Correlation between equilibrium inhibition constant (K_i) and kinetic dissociation constant (k_4/k_3) for unlabeled inhibitors. K_i and k_4/k_3 values are from Table 2 except for TBPS (compound **4**), in which case the kinetic K_d value k_2/k_1 (method C) from Table 1 is used. Correlation coefficients (r) for TBOs, dithianes, and cyclodienes are 0.98, 0.99, and 0.97, respectively.

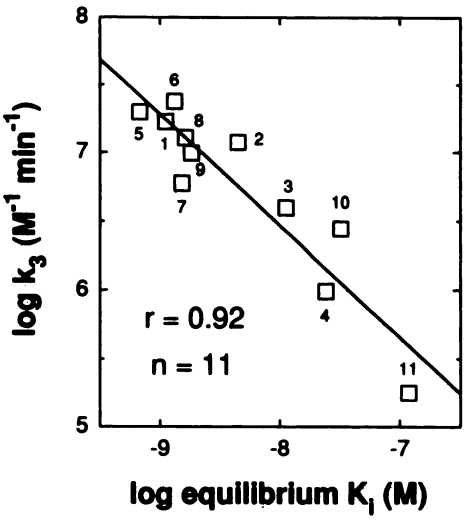

Fig. 6. Correlation between equilibrium inhibition constant (K_i) and association rate constant (k_3) for unlabeled TBOs. K_i and k_3 values are from Table 2 except for TBPS (compound **4**), in which case the association rate k_1 (method C) from Table 1 is used. Correlation coefficient (r) for dithianes is 0.71.

standard method can be at least partially compensated for by using higher radioligand concentrations to increase the k_{obs}.

Dissociation rates for four TBO radioligands. Dissociation studies indicate reversible binding with first-order decay

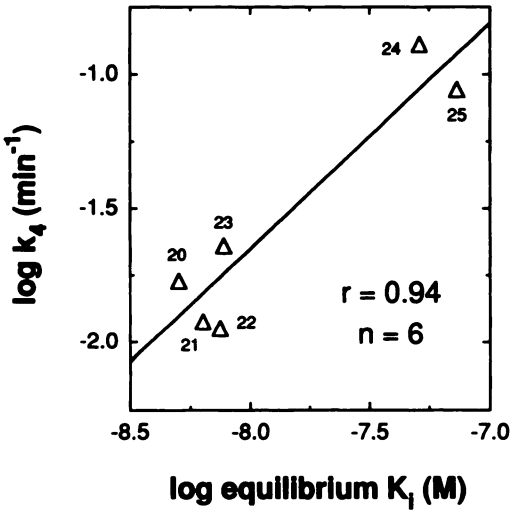

Fig. 7. Correlation between equilibrium inhibition constant (K_i) and dissociation rate constant (k_4) for cyclodienes. K_i and k_4 values are from Table 2. Correlation coefficients (r) for TBOs and dithianes are 0.59 and 0.53, respectively.

for all radioligands (Fig. 3), with rates corresponding to half-lives of 13, 32, 45, and 159 min for [^{3}H]CNsBOB, [^{3}H]TBOB, [^{35}S]TBPS, and [^{3}H]EBOB, respectively. Estimation of the off-rate from the association curve (method C) gives results similar to those from dissociation experiments (method A), with the difference being 1.2–1.4-fold for [^{3}H]CNsBOB, [^{3}H]TBOB, and [^{35}S]TBPS; the divergence for [^{3}H]EBOB is higher (2.3-fold), possibly due to its slow off-rate and/or hydrolysis at pH 7.5 (see below). Largely due to variation in k_1 estimates, the method-dependent differences in estimating values for the kinetic dissociation constant k_2/k_1 are 1.7-, 1.9-, 2.4-, and 3.8-fold for [^{3}H]TBOB, [^{35}S]TBPS, [^{3}H]EBOB, and [^{3}H]CNsBOB, respectively. Methods B and C generally give kinetic estimates of the dissociation constants that are closest to the K_d values derived from Scatchard plots.

Receptor dissociation and buffer hydrolysis rates for orthobenzoate radioligands. The receptor dissociation rate for [^{3}H]EBOB is essentially the same as its hydrolysis rate, i.e., half-life values of 159 ± 25 and 151 ± 2 min, respectively, at pH 7.5. This suggests the possibility that the dissociation might be initiated by EBOB hydrolysis. However, this apparent correlation may be coincidental, based on two other observations. First, a large effect of pH on EBOB hydrolysis rate (half-lives of 28 ± 3 and 646 ± 3 min at pH 6.5 and 8.5, respectively) is not evident in its dissociation rate (data not shown). Second, TBOB and CNsBOB dissociate faster than EBOB at pH 7.5 yet are more stable to hydrolysis under this condition [half lives of >2400 min for TBOB (20) and 1092 ± 39 min for CNsBOB].

Inhibition and kinetic constants for unlabeled ligands. The [^{35}S]TBPS coincubation method for determining kinetic binding constants for unlabeled ligands is illustrated for a representative TBO, dithiane, and cyclodiene in Fig. 4. The decrease in binding of [^{35}S]TBPS with time after an initial peak for EBOB and α-endosulfan is characteristic of ligands with off-rates slower than that of the radioligand (9).

A comparison of the kinetic constants obtained using radioligands (Table 1) and the corresponding unlabeled ligands (Table 2) demonstrates that the [^{35}S]TBPS coincubation method is generally a good predictor of unlabeled ligand kinetics. The kinetics of unlabeled TBPS were not examined because this would, in effect, constitute a radiodilution experiment. On-rates obtained for unlabeled EBOB and TBOB are the same as those for [^{3}H]EBOB and [^{3}H]TBOB (methods B and C), although the estimate for unlabeled CNsBOB is 1.6-fold higher than for [^{3}H]CNsBOB. Off-rates for unlabeled CNsBOB, TBOB, and EBOB using the indirect method differ by 1.3-, 1.8-, and 2.7-fold, respectively, compared with direct determination using the corresponding radioligand (method A). Thus, five of six kinetic constants estimated using the [^{35}S]TBPS coincubation method are within 2.0-fold of the "true" values obtained with radiolabeled forms.

Correlations of equilibrium K_i with kinetic K_d, k_3, and k_4. The very high correlation ($r = 0.98$, $n = 25$; Fig. 5) between the equilibrium K_i values and the kinetically derived K_d values (i.e., k_4/k_3) (Table 2) indicates that the results of [^{35}S]TBPS competition and kinetic coincubation experiments are internally consistent. However, comparison of the equilibrium K_i values obtained from competition experiments with unlabeled ligands and the K_d values for the corresponding radioligands reveals a discrepancy of 1.1-, 1.2-, 1.9-, and 2.6-fold for CNsBOB, TBPS, TBOB, and EBOB, respectively (Tables 1 and 2). Thus, [^{35}S]TBPS coincubation experiments in the presence of unlabeled ligands predict binding kinetics about as well as they predict receptor affinity.

The good correlations between K_i and k_3 for the TBOs ($r = 0.92$, $n = 11$; Fig. 6) and the dithianes ($r = 0.71$, $n = 8$; data not shown) but not between K_i and k_4 ($r = 0.59$ and 0.53, respectively; data not shown) indicate that the affinity of these compounds for the binding site is mainly controlled by the on-rate. Conversely, with the cyclodienes there is a good correlation between K_i and k_4 ($r = 0.94$, $n = 6$; Fig. 7) but not between K_i and k_3 ($r = 0.51$, $n = 6$; data not shown), indicating that the off-rate is a major contributor to affinity for this class of inhibitors.

Discussion

The binding kinetics of three classes of unlabeled inhibitors for the NCB site of the bovine brain $GABA_A$ receptor were determined using the radioligand coincubation method of Contreras *et al.* (10), based on the theory developed by Motulsky and Mahan (9). [^{35}S]TBPS was selected as the radioligand to evaluate the kinetics of unlabeled ligands because of its stability in buffer at pH 7.5, its high specific binding, the close correlations between rate constants determined by different methods and also between kinetic and equilibrium dissociation contants, and its wide use as a probe of the NCB site.

The binding isotherms for the four radioligands studied, with the membrane preparation and incubation conditions used, are indicative of a single population of noninteracting binding sites in bovine cerebral cortex. These findings agree with most of the earlier investigations with [^{35}S]TBPS, [^{3}H]TBOB, and [^{3}H]EBOB; Scatchard and kinetic analyses for [^{3}H]CNsBOB have not been reported previously. Thus, Scatchard analysis of [^{35}S]TBPS saturation experiments gives a straight line, as observed in most (5, 22, 24–27) but not all (28) studies. The K_d and B_{max} values of 20 nM and 1.6 pmol/mg of protein are close to those observed in other studies using KBr in the incubation medium (5, 22). Similarly, the standard transformation of [^{35}S]TBPS association data is monophasic, as observed in other studies

(22, 24, 25, 29, 30). In the present investigation, the dissociation of [^{35}S]TBPS displays monoexponential decay. [^{35}S]TBPS dissociation has been reported to be monophasic (22, 25, 26, 30, 31), biphasic (5, 27, 29, 32), or more complex (28). Scatchard plots of [^{3}H]TBOB binding yield a K_d of 6 nM, similar to that reported by Van Rijn *et al.* (33) but 10-fold lower than in the original report (6), perhaps due to the use of the "cold dilution" approach in the latter study. Linear pseudo-first-order on-rates are observed for [^{3}H]TBOB, consistent with earlier studies (6, 33); however, biphasic instead of monophasic dissociation curves have previously been reported (6, 33). [^{3}H]EBOB is characterized by linear Scatchard and kinetic plots (8). Removal of endogenous GABA and the use of a high salt (e.g., KBr) concentration for optimal binding are apparently important factors resulting in first-order dissociation of radioligands from this binding site.

The apparent uniformity of the NCB binding site in bovine cerebral cortex contrasts with the probable GABA$_A$ receptor heterogeneity. Although the subunit compositions of *in vivo* receptor complexes are unknown, the wide variety of cloned subunit classes, some with multiple isoforms, along with the pharmacologically defined heterogeneity of benzodiazepine receptor sites indicate considerable receptor diversity (34). However, the proposed location for the NCB site in the channel lumen (35) and the high homology of the membrane-spanning regions (34) suggest that the NCB sites of heterogeneous GABA$_A$ receptor complexes may be very similar.

The kinetics of unlabeled ligands were determined by their effect on the [^{35}S]TBPS association curve. This newly validated procedure allowed for the first time the intercomparisons of the binding kinetics of 11 TBOs, eight dithianes, and six cyclodienes.

With the TBOs and dithianes, the on-rate is the main determinant of affinity for the NCB site, based on the good correlation between k_3 and K_i. Fast association rates are conferred by the orthobenzoate versus the phosphorus ester substituents, 4′-ethynyl compared with hydrogen, bromo, or cyano in orthobenzoates, and monosulfone compared with other oxidation states of the dithianes. Slow dissociation rates in the TBOs are associated with ethynyl and bromo compared with cyano and hydrogen substituents. The slow but measurable dissociation of 4′-Br-3′,5′-Cl$_2$-TBOB (half-life, 43 min) is not consistent with the apparent irreversibility of this inhibitor reported previously (14); this discrepancy may be due to its expected high lipophilicity resulting in difficulty in its removal from membranes by the repetitive rinsing procedure used in the earlier study. Compared with the bicycloorthobenzoates (type A action), the reduced on-rate of the phosphorus esters (type B action) explains their low affinity but not their unusually high relative toxicity (36).

The affinities of the cyclodienes, in contrast to those of the TBOs and dithianes, appear to be regulated by the off-rate rather than the on-rate. This finding may indicate that this highly chlorinated, lipophilic, and structurally unrelated class of inhibitors interact with the NCB site in a qualitatively different manner, compared with the TBOs and dithianes.

The on-rates of all ligands examined (range, 0.18 to 26 × 10^6 M^{-1} min^{-1}) are much slower than the diffusion-controlled limit of 6 × 10^{10} M^{-1} min^{-1} (37). The latter value is likely to be an overestimate because the GABA$_A$ receptor is membrane bound and, therefore, diffusionally restricted. However, association rate constants for [^{3}H]muscimol and [^{3}H]flunitrazepam binding to the GABA recognition and benzodiazepine sites of the GABA$_A$ receptor complex present in bovine and rat cortical membranes, respectively, are about 2 × 10^8 M^{-1} min^{-1} (38, 39)[2] at 0° and would be faster at 25°, as used in the present study. The slow association of NCB site ligands suggests that binding is a two-step process. This might involve an initial partitioning into the membrane or a conformational change of the receptor complex associated with ligand binding. The first possibility predicts a correlation between membrane partitioning and on-rate, which is not immediately obvious in preliminary consideration of the ligand structures. The latter option, therefore, warrants further consideration.

The binding affinity of these ligands is closely correlated with their inhibition of $^{36}Cl^-$ flux and thus is a good indicator of chloride channel block (4). On this basis, the slow overall association rates are consistent with binding to a slowly forming blocked conformation of the receptor in the absence of GABA. This interpretation is supported by the slow onset (without GABA pretreatment) of the TBPS-induced block of GABA-evoked currents in *Xenopus* oocytes injected with chick brain mRNA (40). The on-rate-controlled affinity for the TBOs and dithianes suggests a lock-and-key model in which the ligand on-rate is proportional to the rate at which the receptor assumes the blocked conformation. As an alternative, an induced-fit model is also plausible, in which ligands with higher on-rates increase the rate of conformational change. Although the data cannot discriminate between these two possibilities, the induced-fit model is favored because it explains protein-ligand interactions in most systems (41).

Acknowledgments

We thank Christopher Palmer and Vincent Wacher for providing the TBOs and dithianes, respectively, and Wing-Wah Lam for NMR analysis of the TBOs.

References

1. Casida, J. E., L. M. Cole, J. E. Hawkinson, and C. J. Palmer. Trioxabicyclooctanes: GABA receptor binding site and comparative toxicology. *R. Soc. Chem. Spec. Publ.* **79**:212–234 (1990).
2. Hawkinson, J. E., and J. E. Casida. Insecticide binding sites on GABA receptors of insects and mammals. *Am. Chem. Soc. Symp. Ser.*, in press.
3. Casida, J. E. Insecticide action at the GABA-gated chloride channel: recognition, progress and prospects. *Arch. Insect Biochem. Physiol.*, in press.
4. Obata, T., H. I. Yamamura, E. Malatynska, M. Ikeda, H. Laird, C. J. Palmer, and J. E. Casida. Modulation of γ-aminobutyric acid-stimulated chloride influx by bicycloorthocarboxylates, bicyclophosphorus esters, polychlorocycloalkanes and other cage convulsants. *J. Pharmacol. Exp. Ther.* **244**:802–806 (1988).
5. Squires, R. F., J. E. Casida, M. Richardson, and E. Saederup. [^{35}S]*t*-Butylbicyclophosphorothionate binds with high affinity to brain-specific sites coupled to γ-aminobutyric acid-A and ion recognition sites. *Mol. Pharmacol.* **23**:326–336 (1983).
6. Lawrence, L. J., C. J. Palmer, K. W. Gee, X. Wang, H. I. Yamamura, and J. E. Casida. *t*-[^{3}H]Butylbicycloorthobenzoate: new radioligand probe for the γ-aminobutyric acid-regulated chloride ionophore. *J. Neurochem.* **45**:798–804 (1985).
7. Nicholson, R. A., C. J. Palmer, R. F. Toia, and J. E. Casida. 4-*s*-[^{3}H]Butyl-1-(4-cyanophenyl)-2,6,7-trioxabicyclo[2.2.2]octane: specific binding in the cockroach central nervous system. *Pestic. Sci.* **24**:183–185 (1988).
8. Cole, L. M., and J. E. Casida. GABA-gated chloride channel: binding site for 4′-ethynyl-4-*n*-[2,3-^{3}H$_2$]propylbicycloorthobenzoate ([^{3}H]EBOB) in vertebrate brain and insect head. *Pestic. Biochem. Physiol.*, **44**:1–8 (1992).
9. Motulsky, H. J., and L. C. Mahan. The kinetics of competitive radioligand binding predicted by the law of mass action. *Mol. Pharmacol.* **25**:1–9 (1984).
10. Contreras, M. L., B. B. Wolfe, and P. B. Molinoff. Kinetic analysis of the interactions of agonists and antagonists with *beta* adrenergic receptors. *J. Pharmacol. Exp. Ther.* **239**:136–143 (1986).

[2] The association rate constant for [^{3}H]flunitrazepam (2 nM) was calculated, using eq. 5, from k_{obs} (0.469 min^{-1}) and k_2 (0.1115 min^{-1}) for the fast kinetic phase (38); k_1 for [^{3}H]muscimol was calculated from 3.6 × 10^6 M^{-1} sec^{-1} for the slow phase (39).

11. Palmer, C. J., and J. E. Casida. Novel selective catalytic reduction with tritium: synthesis of the $GABA_A$ receptor radioligand 1-(4-ethynylphenyl)-4-[2,3-$^3H_2$]propyl-2,6,7-trioxabicyclo[2.2.2]octane. *J. Labelled Compd. Radiopharm.* **29**:829–839 (1991).
12. Milbrath, D. S., J. L. Engel, J. G. Verkade, and J. E. Casida. Structure-toxicity relationships of 1-substituted-4-alkyl-2,6,7-trioxabicyclo[2.2.2]octanes. *Toxicol. Appl. Pharmacol.* **47**:287–293 (1979).
13. Casida, J. E., C. J. Palmer, and L. M. Cole. Bicycloorthocarboxylate convulsants: potent $GABA_A$ receptor antagonists. *Mol. Pharmacol.* **28**:246–253 (1985).
14. Hawkinson, J. E., M. P. Goeldner, C. J. Palmer, and J. E. Casida. Photoaffinity ligands for the [^{3}H]TBOB binding site of the $GABA_A$ receptor. *J. Recept. Res.* **11**:391–405 (1991).
15. Palmer, C. J., L. M. Cole, and J. E. Casida. (±)-4-*tert*-Butyl-3-cyano-1-(4-ethynylphenyl)-2,6,7-trioxabicyclo[2.2.2]octane: synthesis of a remarkably potent $GABA_A$ receptor antagonist. *J. Med. Chem.* **31**:1064–1066 (1988).
16. Palmer, C. J., L. M. Cole, J. P. Larkin, I. H. Smith, and J. E. Casida. 1-(4-Ethynylphenyl)-4-substituted-2,6,7-trioxabicyclo[2.2.2]octanes: effect of 4-substituent on toxicity to houseflies and mice and potency at the GABA-gated chloride channel. *J. Agric. Food Chem.* **39**:1329–1334 (1991).
17. Palmer, C. J., and J. E. Casida. 1-(4-Ethynylphenyl)-2,6,7-trioxabicyclo[2.2.2]octanes: a new order of potency for insecticides acting at the GABA-gated chloride channel. *J. Agric. Food Chem.* **37**:213–216 (1989).
18. Wacher, V. J., R. F. Toia, and J. E. Casida. 2-Aryl-5-*tert*-butyl-1,3-dithianes and their *S*-oxidation products: structure-activity relationships of potent insecticides acting at the GABA-gated chloride channel. *J. Agric. Food Chem.* **40**:497–505 (1992).
19. Lawrence, L. J., and J. E. Casida. Interactions of lindane, toxaphene and cyclodienes with brain-specific *t*-butylbicyclophosphorothionate receptor. *Life Sci.* **35**:171–178 (1984).
20. Scott, J. G., C. J. Palmer, and J. E. Casida. Oxidative metabolism of the $GABA_A$ receptor antagonist *t*-butylbicycloortho[^{3}H]benzoate. *Xenobiotica* **17**:1085–1093 (1987).
21. Peterson, G. L. A simplification of the protein assay method of Lowry *et al.* which is more generally applicable. *Anal. Biochem.* **83**:346–356 (1977).
22. Garrett, K. M., A. J. Blume, and M. S. Abel. Effect of halide ions on *t*-[^{35}S]butylbicyclophosphorothionate binding. *J. Neurochem.* **53**:935–939 (1989).
23. Cheng, Y.-C., and W. H. Prusoff. Relationship between the inhibition constant (K_i) and the concentration of inhibitor which causes 50 per cent inhibition (I_{50}) of an enzymatic reaction. *Biochem. Pharmacol.* **22**:3099–3108 (1973).
24. Cole, L. M., L. J. Lawrence, and J. E. Casida. Similar properties of [^{35}S]*t*-butylbicyclophosphorothionate receptor and coupled components of the GABA receptor-ionophore complex in brains of human, cow, rat, chicken and fish. *Life Sci.* **35**:1755–1762 (1984).
25. Seifert, J., and J. E. Casida. Regulation of [^{35}S]*t*-butylbicyclophosphorothionate binding sites in rat brain by GABA, pyrethroid and barbiturate. *Eur. J. Pharmacol.* **115**:191–198 (1985).
26. Trifiletti, R. R., A. M. Snowman, and S. H. Snyder. Barbiturate recognition site on the GABA/benzodiazepine receptor complex is distinct from the picrotoxinin/TBPS recognition site. *Eur. J. Pharmacol.* **106**:441–447 (1984).
27. Trifiletti, R. R., A. M. Snowman, and S. H. Snyder. Anxiolytic cyclopyrrolone drugs allosterically modulate the binding of [^{35}S]*t*-butylbicyclophosphorothionate to the benzodiazepine/γ-aminobutyric acid-A receptor/chloride ionophore complex. *Mol. Pharmacol.* **26**:470–476 (1984).
28. Tehrani, M. H. J., C. J. Clancey, and E. M. Barnes, Jr. Multiple [^{35}S]*t*-butylbicyclophosphorothionate binding sites in rat and chicken cerebral hemispheres. *J. Neurochem.* **45**:1311–1314 (1985).
29. Maksay, G., and M. Simonyi. Kinetic regulation of convulsant (TBPS) binding by GABAergic agents. *Mol. Pharmacol.* **30**:321–328 (1986).
30. Maksay, G., and M. K. Ticku. Dissociation of [^{35}S]*t*-butylbicyclophosphorothionate binding differentiates convulsant and depressant drugs that modulate GABAergic transmission. *J. Neurochem.* **44**:480–486 (1985).
31. Gee, K. W., D. S. Joy, and D. Belelli. Complex interactions between pregnenolone sulfate and the *t*-butylbicyclophosphorothionate-labeled chloride ionophore in rat brain. *Brain Res.* **482**:169–173 (1989).
32. Gee, K. W., L. J. Lawrence, and H. I. Yamamura. Modulation of the chloride ionophore by benzodiazepine receptor ligands: influence of γ-aminobutyric acid and ligand efficacy. *Mol. Pharmacol.* **30**:218–225 (1986).
33. Van Rijn, C. M., E. Willems-van Bree, T. J. A. M. Van der Velden, and J. F. Rodrigues de Miranda. Binding of the cage convulsant, [^{3}H]TBOB, to sites linked to the $GABA_A$ receptor complex. *Eur. J. Pharmacol.* **179**:419–425 (1990).
34. Olsen, R. W., and A. J. Tobin. Molecular biology of $GABA_A$ receptors. *FASEB J.* **4**:1469–1480 (1990).
35. Havoundjian, H., S. M. Paul, and P. Skolnick. The permeability of γ-aminobutyric acid-gated chloride channels is described by the binding of a "cage" convulsant, *t*-butylbicyclophosphoro[^{35}S]thionate. *Proc. Natl. Acad. Sci. USA* **83**:9241–9244 (1986).
36. Palmer, C. J., and J. E. Casida. Two types of cage convulsant action at the GABA-gated chloride channel. *Toxicol. Lett.* **42**:117–122 (1988).
37. Fersht, A. *Enzyme Structure and Mechanism*. W. H. Freeman and Co., New York, 150 (1977).
38. Chiu, T. H., D. M. Dryden, and H. C. Rosenberg. Kinetics of [^{3}H]flunitrazepam binding to membrane-bound benzodiazepine receptors. *Mol. Pharmacol.* **21**:57–65 (1982).
39. Agey, M. W., and S. M. J. Dunn. Kinetics of [^{3}H]muscimol binding to the $GABA_A$ receptor in bovine brain membranes. *Biochemistry* **28**:4200–4208 (1989).
40. Van Renterghem, C., G. Bilbe, S. Moss, T. G. Smart, A. Constanti, D. A. Brown, and E. A. Barnard. GABA receptors induced in *Xenopus* oocytes by chick brain mRNA: evaluation of TBPS as a use-dependent channel-blocker. *Mol. Brain Res.* **2**:21–31 (1987).
41. Jorgensen, W. L. Rusting of the lock and key model for protein-ligand binding. *Science* (Washington, D. C.) **254**:954–955 (1991).
42. Hawkinson, J. E., and J. E. Casida. Insecticide Kinetics at the $GABA_A$ receptor noncompetitive blocker binding site. *Toxicologist* **12**:292 (1992).

Send reprint requests to: Dr. John E. Casida, Pesticide Chemistry and Toxicology Laboratory, Department of Entomological Sciences, University of California, Berkeley, CA 94720.